Science Advances
AAAS

advances.sciencemag.org/cgi/content/full/6/25/eaba2187/DC1

Supplementary Materials for

LiQD Cornea: Pro-regeneration collagen mimetics as patches and alternatives to corneal transplantation

Christopher D. McTiernan, Fiona C. Simpson, Michel Haagdorens, Chameen Samarawickrama, Damien Hunter, Oleksiy Buznyk, Per Fagerholm, Monika K. Ljunggren, Philip Lewis, Isabel Pintelon, David Olsen, Elle Edin, Marc Groleau, Bruce D. Allan*, May Griffith*

*Corresponding author. Email: may.griffith@umontreal.ca (M. Griffith); bruce.allan@ucl.ac.uk (B.D.A.)

Published 17 June 2020, *Sci. Adv.* **6**, eaba2187 (2020)
DOI: 10.1126/sciadv.aba2187

This PDF file includes:

Supplementary Materials

Supplementary Notes

Note S1. Towards point-of-care (POC) delivery of LiQD Cornea.

Currently, LiQD Cornea is prepared through multi-component mixing in a T-piece syringe mixing system (Fig. S3A.) fitted with an injection port through which the DMTMM crosslinking solution is added. Upon addition of the crosslinking solution the material is mixed until homogenous by alternating depression of the two attached syringe plungers. Once mixed the T-piece system is disassembled and the material is applied to the wound bed by dispensing the material from the glass syringe. Although this method provides adequate mixing and materials that are free of bubbles, it is a labor-intensive process that requires multiple mixing and addition steps which adds complexity to an already difficult procedure and may require specialized training or additional personnel.

In order to simplify the preparation and application of LiQD Cornea to the wound bed in the clinical setting we have begun to explore a variety of different POC delivery systems which would allow the various components of the formulation to be prepackaged, shipped and stored separately under appropriate conditions as "cartridges". These cartridges would then be inserted into a simple delivery/mixing device that requires nothing more than the depression of a plunger to obtain adequate mixing and dispersal of the material into the wound bed. One such POC delivery system is depicted in Fig. S3B. In this dual syringe system, one syringe is filled with a solution comprised of 10% CLP-PEG and 1% fibrinogen w/w while the other is filled with 10% w/w DMTMM in 10 mM PBS. The syringes are attached through a dual syringe adapter (Medmix Systems AG, Switzerland), which was fitted with a static mixer (Medmix Systems AG, Switzerland) and a 19 G x 25 mm flattened tip cannula. After heating the system to 50 ºC, the dual plunger of the delivery system is depressed and the contents of the two syringes are mixed in a 1:1 ratio through the microfluidics based static mixer before exiting the device from a 19 G cannula. Application of LiQD Cornea to an *ex vivo* corneal perforation model utilizing the POC device resulted in its filling and formation of a seal (Fig. S3C, S3D), however the resulting seal was weaker with an average bursting pressure of 93 ± 20 mmHg. While this bursting pressure is lower than that measured for the material prepared using the T-piece system, it is important to point out that this pressure is still well above the average intraocular pressure of the human eye and due to the 1:1 mixing ratio of the two components in the POC delivery system the nominal solid content of the dispensed filler is decreased from approximately 9.5% in the T-piece system to 6% in the POC system. Thus, while this preliminary POC delivery device illustrates the feasibility of delivering LiQD Cornea via a simple delivery system, further optimization with regards to component concentration, mixing ratio, and static mixing devices may be required.

Supplementary Figures

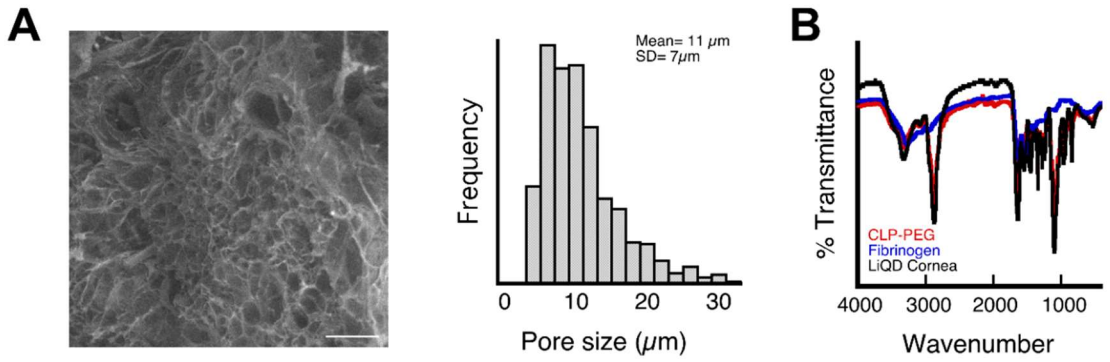

Figure S1. Cryo-scanning electron microscopy (SEM) and Fourier-transform infrared spectroscopy (FTIR) of LiQD Cornea hydrogels. (A) Representative cryo-SEM image of the LiQD cornea and corresponding pore size histogram, which illustrates the mean pore size of the resulting hydrogel. Mean was determined from the measurement of > 250 different pores. Scale bar, 50 μm. (B) Overlay of the representative ATR-FTIR spectra of CLP-PEG (red), fibrinogen (blue), and crosslinked LiQD Cornea (black). The characteristic amide peaks of both the CLP-PEG conjugate and fibrinogen are present in the crosslinked LiQD cornea.

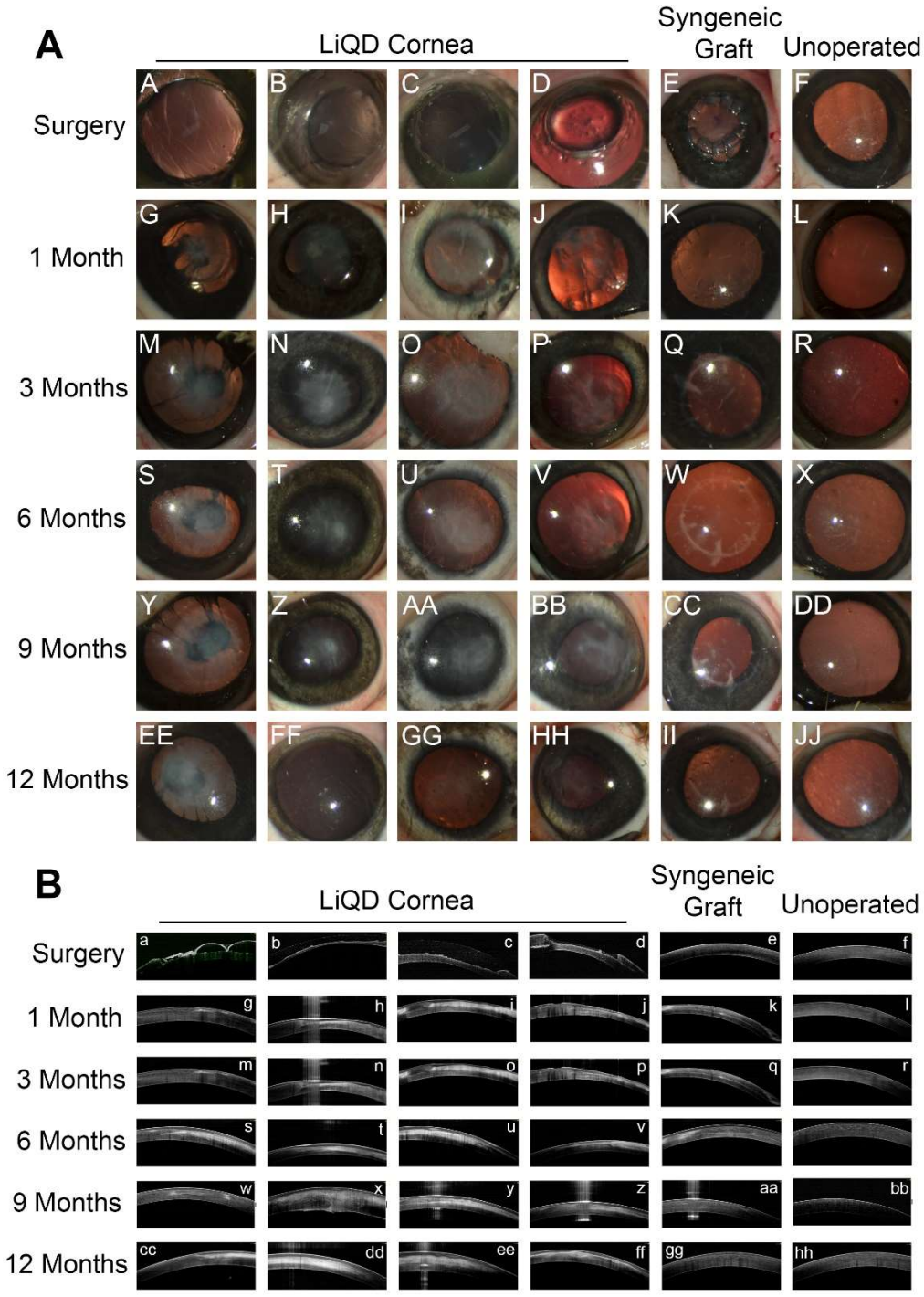

Figure S2. Clinical progression of the LiQD Cornea in all four Göttingen mini-pigs. (A) Surgical microscope images showing the presence of haze at 3 months post-surgery as stromal cells are migrating into the implant. The haze is diminished at 12 months except in one animal where an unintended perforation and suture placement resulted in haze. Representative images of a syngeneic corneal graft and an untreated contralateral cornea are shown as controls. Haze is seen at the graft-host interface of the syngeneic cornea. Photo Credit: Monika K. Ljunggren, Linköping University. (B) Optical coherence tomography images of representative samples of LiQD Cornea, syngeneic grafts and unoperated corneas over 12 months post-surgery. The filling of the surgical wound bed was not always optimal as shown by the over-filled LiQD Cornea that had gelled *in situ* (a). Remodeling over the initial 3 months resulted in a regenerated cornea with a smooth external

curvature that conforms to the overall shape of the host cornea (p). The initially cell-free hydrogel (a-d) became populated with cells (m-p, s-v, w-z, cc-ff).

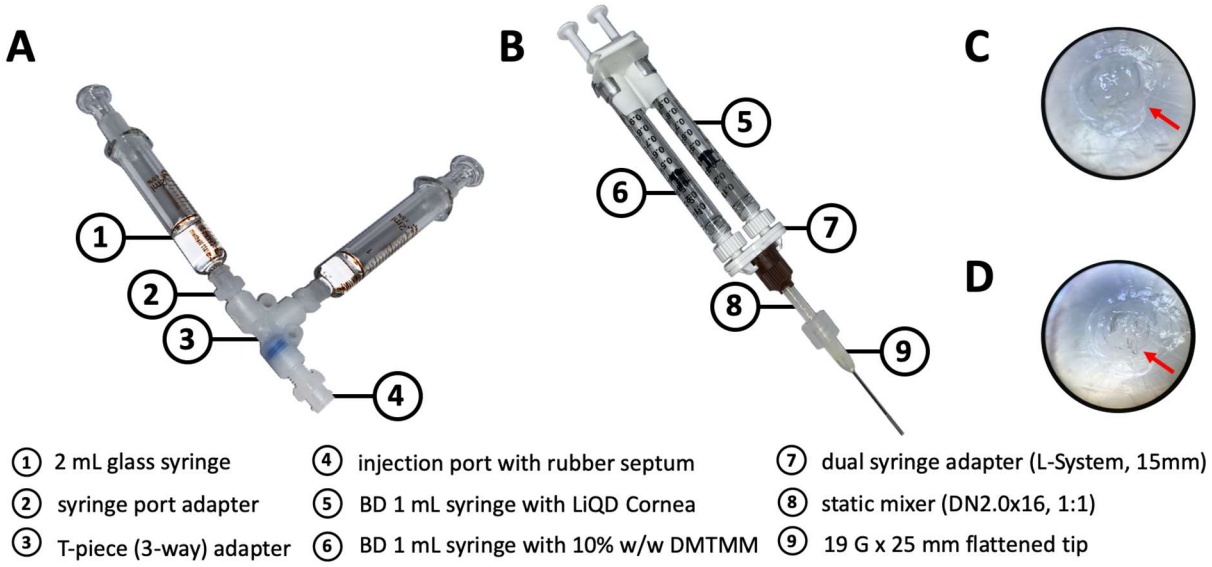

Figure S3. Towards point-of-care (POC) delivery of LiQD Cornea. Comparison of the current T-piece mixing system (A) with the preliminary POC delivery system (B). (C) Representative image of an *ex-vivo* perforation model sealed using LiQD Cornea that was mixed and dispensed to the wound bed using the preliminary POC delivery system. (D) POC delivered LiQD Cornea after failure in bursting pressure testing. Red arrows indicate the interface of the applied material and the perforated cornea. Photo Credit: Christopher D. McTiernan, Université de Montréal.

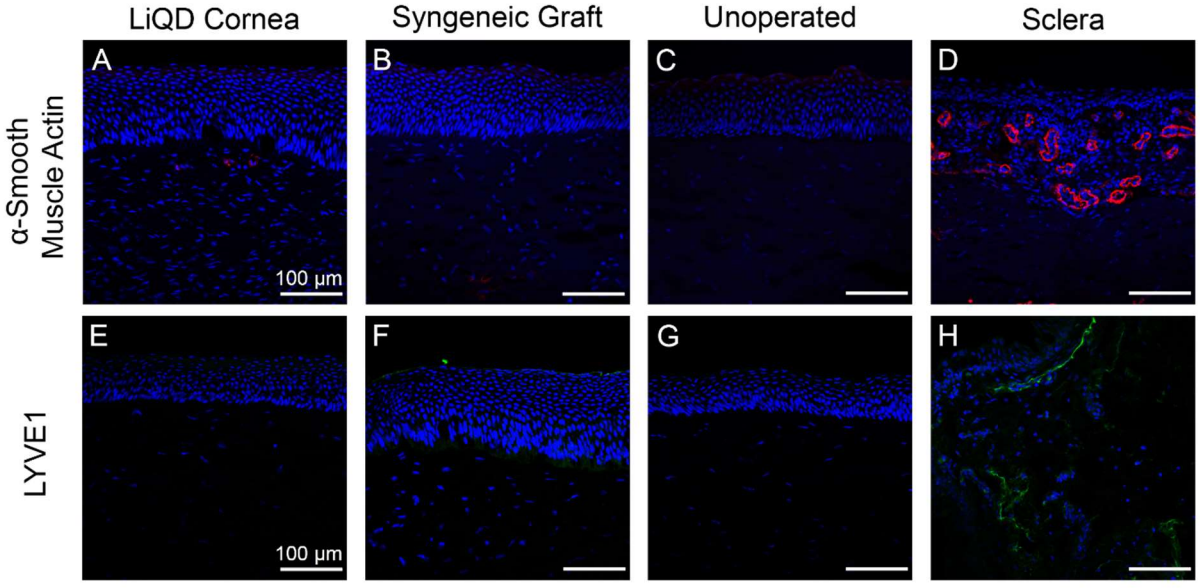

Figure S4. Immunohistochemistry of the cornea at 12 months. (A-C) The operated corneas show minimal staining for α-SMA, and no large vessels present in the operated region although they are present in the scleral positive control (D). (E-G) LYVE1 was not observed in the central cornea, although lymphatic vessels were seen in the corneal limbus and sclera (H). Cell nuclei were stained blue with DAPI.

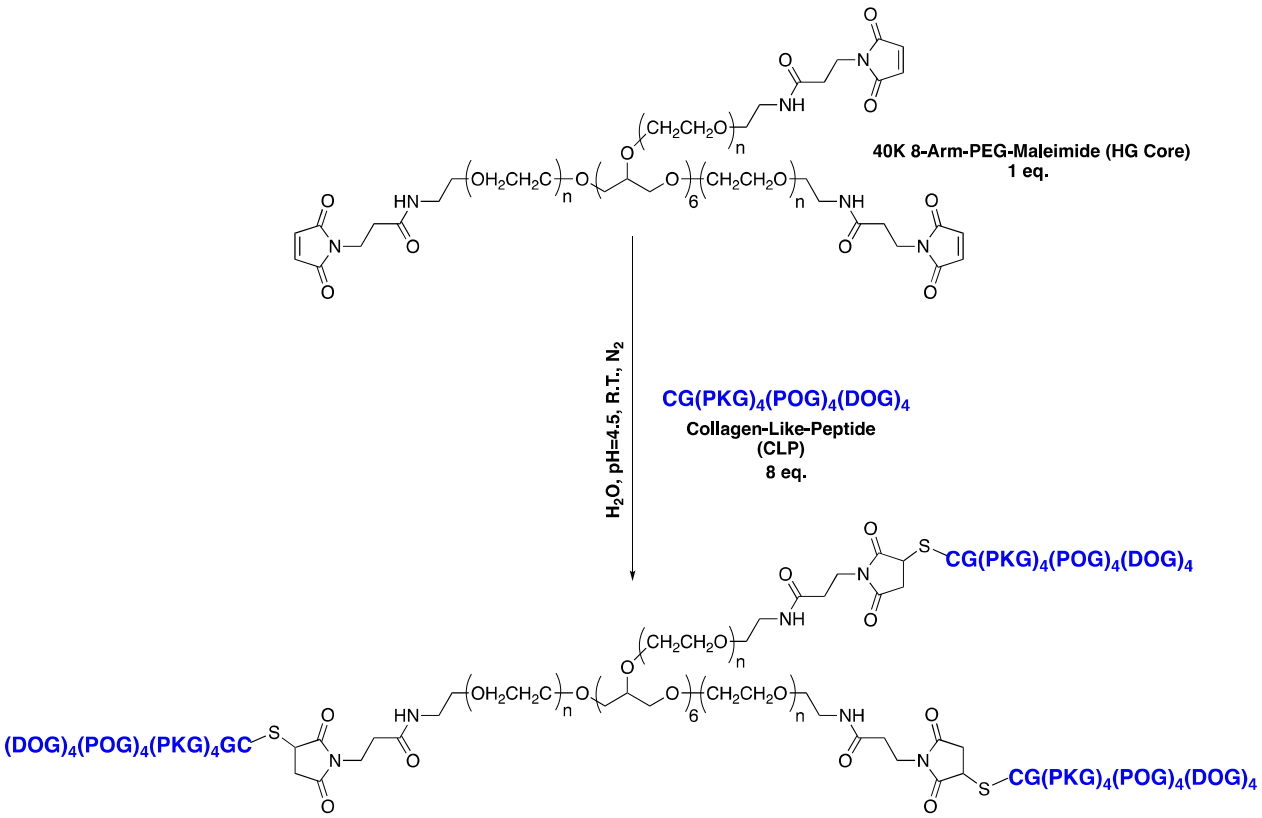

Figure S5. Schematic for the preparation of CLP-PEG conjugate.

Supplementary Tables

Table S1. Antibodies for Immunocytochemistry

Target	**Antibody (or Lectin)**	**Dilution Factor**
CD206	Anti-Mannose Receptor antibody, AbCam, ab64693	1/1000
CD86	Anti-CD86 antibody [GL-1], AbCam, ab119857	1/500
Rat IgG	Donkey anti-rat IgG (H+L) Highly Cross-Adsorbed Secondary Antibody, Alexa Fluor 488 (Invitrogen, A-21208)	1/2000
Rabbit IgG	Goat anti-Rabbit IgG (H+L) Cross-Adsorbed Secondary Antibody, Alexa Fluor 568 (Invitrogen, A-11011)	1/2000

Table S2. Antibodies for Immunohistochemistry

Target	**Antibody (or Lectin)**	**Dilution Factor**
Mucin	Lectin from Ulex europaeus (gorse, furze) FITC conjugate, Sigma-Aldrich, L9006	1/500
Cytokeratin 12	Recombinant Anti-Keratin 12/K12 antibody [EPR17882], AbCam, ab185627	1/500
α-SMA	Anti-alpha smooth muscle Actin antibody [1A4], AbCam, ab7817	1/500
LYVE1	Anti-LYVE1 antibody, AbCam, ab33682	1/100
CD163	CD163 antibody | 2A10/11, Bio-Rad, MCA2311GA	1/500
B3-tubulin	beta Tubulin Antibody, Novus Biologicals, NB-600-936	1/1000
CD31	Anti-CD31 antibody [C31.3 + JC/70A]. AbCam, ab199012	1/500
CD9	CD9 Mouse anti-Bovine, Canine, Equine, Feline, Human, Mink, Mustelid, Non-human primate, Porcine, Rabbit, Clone: MM2/57, Invitrogen™, MA180307	1/100
Tsg101	Recombinant Anti-TSG101 antibody [EPR7130(B)], AbCam, ab125011	1/100
Mouse IgG	IgG (H+L) Highly Cross-Adsorbed Goat anti-Mouse, Alexa Fluor® 488, Invitrogen, A11029	1/1000
Rabbit IgG	IgG (H+L) Highly Cross-Adsorbed Goat anti-Rabbit, Alexa Fluor® 594, Invitrogen, A11037	1/1000
Mouse IgG	IgG (H+L) Highly Cross-Adsorbed Goat anti-Mouse, Alexa Fluor® Plus 647, Invitrogen™, PIA32728	1/1000

Table S3. Antibodies for Flow Cytometry

Target	**Antibody**	**Dilution Factor**
CD11c	Brilliant Violet 650™ anti-mouse CD11c,(Clone: N418),(IsoType: Armenian Hamster IgG),(Reactivity: Mouse),(Format: BV650),(APP: FC),(Species: Hamster), Biolegend, 117339	1/1600
IA-IE (MHC Class II)	PerCP/Cy5.5 anti-mouse I-A/I-E,(Clone: M5/114.15.2),(IsoType: Rat IgG2b, κ),(Reactivity: Mouse),(Format: PerCP/Cy5.5),(APP: FC),(Species: Rat), Biolegend, 107626	1/3200
CD40	CD40, APC, clone: 1C10, eBioscience™, 501129392	1/400
CD80	PE anti-mouse CD80,(Clone: 16-10A1),(IsoType: Armenian Hamster IgG),(Reactivity: Mouse, Cross-Reactivity: Dog (Canine)),(Format: PE),(APP: FC),(Species: Hamster), Biolegend, 104708	1/100
CD86	FITC anti-mouse CD86,(Clone: GL-1),(IsoType: Rat IgG2a, κ),(Reactivity: Mouse),(Format: FITC),(APP: FC),(Species: Rat), Biolegend, 105006	1/50

Table S4. Clinical Results – Mixed-effects model

Pachymetry			
Fixed effects (type III)	**P value**	**F (DFn, DFd)**	**Geisser-Greenhouse's epsilon**
Time	0.0045	F (1.830, 23.79) = 7.150	0.4575
Treatment	0.3941	F (2, 13) = 1.001	
Time x Treatment	0.2117	F (8, 52) = 1.417	
Random effects	**SD**	**Variance**	
Pig	73.13	5348	
Residual	47.1	2218	
Was the matching effective?		Chi-square, df	12.06, 1
		P value	0.0005
IOP			
Fixed effects (type III)	**P value**	**F (DFn, DFd)**	**Geisser-Greenhouse's epsilon**
Time	<0.0001	F (3.682, 47.87) = 11.68	0.7365
Treatment	0.6255	F (2, 13) = 0.4866	
Time x Treatment	0.0943	F (10, 65) = 1.723	
Random effects	**SD**	**Variance**	
Pig	1.342	1.801	
Residual	2.342	5.486	
Was the matching effective?		Chi-square, df	7.991, 1
		P value	0.0047
Haze			
Fixed effects (type III)	**P value**	**F (DFn, DFd)**	**Geisser-Greenhouse's epsilon**
Time	0.0002	F (2.661, 34.59) = 9.092	0.5322
Treatment	<0.0001	F (2, 13) = 47.40	
Time x Treatment	<0.0001	F (10, 65) = 6.769	
Random effects	**SD**	**Variance**	
Pig	0.1826	0.03333	
Residual	0.3232	0.1045	
Was the matching effective?		Chi-square, df	7.693, 1
		P value	0.0055

Implant Neovascularization			
Fixed effects (type III)	**P value**	**F (DFn, DFd)**	**Geisser-Greenhouse's epsilon**
Time	0.0186	F (2.444, 31.77) = 4.173	0.4887
Treatment	0.0055	F (2, 13) = 7.977	
Time x Treatment	0.0041	F (10, 65) = 2.949	
Random effects	**SD**	**Variance**	
Pig	0.4974	0.2474	
Residual	0.4557	0.2077	
Was the matching effective?		Chi-square, df	33.92, 1
		P value	<0.0001
Aesthesiometry			
Fixed effects (type III)	**P value**	**F (DFn, DFd)**	**Geisser-Greenhouse's epsilon**
Time	0.0207	F (1.019, 7.136) = 8.702	0.3398
Treatment	0.2408	F (1.311, 9.178) = 1.631	0.6556
Time x Treatment	0.2251	F (2.080, 1.734) = 3.999	0.3467
Random effects	**SD**	**Variance**	
Pig	0.1652	0.0273	
Pig x Time	0	0	
Pig x Treatment	0.2884	0.08317	
Residual	0.5188	0.2691	
Was the matching effective?		Chi-square, df	5.236, 2
		P value	0.0729
Nerve Density			
Fixed effects (type III)	**P value**	**F (DFn, DFd)**	**Geisser-Greenhouse's epsilon**
Time	0.0243	F (2.773, 34.67) = 3.653	0.6933
Treatment	0.0033	F (2, 13) = 9.160	
Time x Treatment	0.0745	F (8, 50) = 1.939	
Random effects	**SD**	**Variance**	
Pig	309.9	96028	
Residual	1275	1625511	
Was the matching effective?		Chi-square, df	0.3532, 1
		P value	0.5523

Schirmer's Tear Test			
Fixed effects (type III)	**P value**	**F (DFn, DFd)**	**Geisser-Greenhouse's epsilon**
Time	0.1752	F (3.187, 41.44) = 1.719	0.4575
Treatment	0.796	F (2, 13) = 0.2322	
Time x Treatment	0.7514	F (10, 65) = 0.6660	
Random effects	**SD**	**Variance**	
Subject	73.13	10.64	
Residual	47.1	23.51	
Was the matching effective?		Chi-square, df	12.06, 1
		P value	0.0005

Table S5. Collagen Content One-Way ANOVAs

		Sum of Squares	df	Mean Square	F	Sig.
HMW	Between Groups	3.89E+11	2	1.94E+11	3.707	0.053
	Within Groups	6.82E+11	13	5.25E+10		
	Total	1.07E+12	15			
γ	Between Groups	1.26E+12	2	6.30E+11	14.922	0.000
	Within Groups	5.49E+11	13	4.22E+10		
	Total	1.81E+12	15			
β	Between Groups	9.61E+12	2	4.80E+12	28.254	0.000
	Within Groups	2.21E+12	13	1.70E+11		
	Total	1.18E+13	15			
α1(V)	Between Groups	1.11E+11	2	5.56E+10	6.479	0.011
	Within Groups	1.12E+11	13	8.59E+09		
	Total	2.23E+11	15			
α 1(I)	Between Groups	3.17E+12	2	1.59E+12	8.498	0.004
	Within Groups	2.43E+12	13	1.87E+11		
	Total	5.60E+12	15			
α2(I)	Between Groups	5.90E+11	2	2.95E+11	2.729	0.102
	Within Groups	1.40E+12	13	1.08E+11		
	Total	1.99E+12	15			

df – degrees of freedom